mouse ES cell line CJ7 was done as described (*19*). Correctly targeted ES cell clones were injected into C57BL/6 blastocysts, and chimeras were bred with C57BL/6 and 129/Sv mice to generate heterozygous animals (*19*). Targeting of the $G\alpha_{13}$ gene and germline transmission of the targeted allele were confirmed by Southern blotting. ES cell DNA or tail DNA from litters of F_1 were digested with Sma I and hybridized with the diagnostic probe from a 5′ external upstream region, a 0.4-kb Sma I to Eco RI fragment.

23. Total RNA was purified from the embryo proper or from the yolk sac and reverse-transcribed with random primers and Moloney murine leukemia virus reverse transcriptase (Gibco BRL). Oligonucleotides used for PCR reaction were for $G\alpha_{13}$ (AGCAGCGCAAGTCCAAGGAGATCG and AGGAACACTCGAGTCTCCACCATCC), $G\alpha_{12}$ (TCAAGCAGATGCGCATCATCCACG and AACTCGCTTCTGCGGCTGAAGGC), and $G\alpha_q$ (GCCATGATCAGAGCGATGGACACG and CTGGGAAGTAGTCGACTAGGTGGG). Primer sequences were chosen so that primers hybridized to DNA regions encoded by different exons (*7*) in order to distinguish cDNA-dependent amplification from amplification of genomic DNA.
24. Whole mount immunohistostaining procedure was adapted from (*20*). Detergent was omitted from every step, and the entire procedure was performed at room temperature. Dissected yolk sacs were fixed in 4% paraformaldehyde, stored in methanol, and rehydrated before immunostaining. After incubation for 1 hour with dry milk (3% w/v), yolk sacs were incubated for another hour with anti–PECAM-1 (rat monoclonal antibody MEC 13.3, Pharmingen; 20 μg/ml), washed, and incubated for about 40 min with alkaline phosphatase–conjugated goat anti-rat immunoglobulin G (Sigma). Yolk sacs were washed extensively, and color reaction was started by addition of 5-bromo-4-chloro-3-indoyl phosphate (BCIP) and nitro blue tetrazolium (NBT). The reaction was stopped after about 30 min.
25. Embryos were fixed in glutaraldehyde and OsO_4, embedded in Epon, sectioned at 0.5 μm, and stained with toluidin blue.
26. Embryonic cells were prepared and cultured from E8.5 embryos as described (*13*). Inositol phosphate production and [^{3}H]thymidine incorporation of serum-starved cells were determined as described (*21*).
27. For examination of cell migration, cells were serum-starved for 24 hours and migration was quantified by a microchamber technique. Cell suspensions (1×10^6 cells/ml) and stimuli were prepared in serum-free Dulbecco's minimum essential medium. Stimuli or control solutions (30 μl) were placed in the lower compartment of a 48-well migration chamber (NeuroProbe). Wells were overlaid with a polycarbonate membrane (pore size, 8 μm; NeuroProbe), and 50 μl of cell suspension was added to the top well. Chambers were incubated for 16 hours at 37°C, then membranes were removed, fixed in methanol, and stained with hematoxylin. We quantified cells that had migrated through the filter by counting six nonoverlaping fields at 200× magnification. To determine whether the migration of cells in response to thrombin was chemotactic or chemokinetic, we performed checkerboard experiments (*7*). In the presence of a negative ligand gradient (higher concentration on the cellular site), there was still migration of cells on the upper site of the filter (about 60 to 70% compared to positive gradient conditions). Equal concentrations of thrombin on both sites resulted in cell migration comparable to that under a positive gradient, indicating that the observed migration was predominantly chemokinetic.
28. We thank J. Edens, Y.-H. Hu, and the La Jolla Cancer Research Foundation for technical assistance; T. Gridley for ES cell line CJ7; and A. Aragay, S. Pease, H. Wang, T. Wieland, and J. T. Yang for helpful suggestions. Supported by NIH grants GM 34236 and AG 12288 (M.I.S.). S.O. was a recipient of a fellowship from the Deutsche Forschungsgemeinschaft and the Guenther Foundation.

9 September 1996; accepted 2 December 1996

DCP-1, a *Drosophila* Cell Death Protease Essential for Development

Zhiwei Song, Kimberly McCall, Hermann Steller*

Apoptosis, a form of cellular suicide, involves the activation of CED-3–related cysteine proteases (caspases). The regulation of caspases by apoptotic signals and the precise mechanism by which they kill the cell remain unknown. In *Drosophila*, different death-inducing stimuli induce the expression of the apoptotic activator *reaper*. Cell killing by *reaper* and two genetically linked apoptotic activators, *hid* and *grim*, requires caspase activity. A *Drosophila* caspase, named *Drosophila* caspase-1 (DCP-1), was identified and found to be structurally and biochemically similar to *Caenorhabditis elegans* CED-3. Loss of zygotic DCP-1 function in *Drosophila* caused larval lethality and melanotic tumors, showing that this gene is essential for normal development.

Programmed cell death, or apoptosis, is of fundamental importance for the elimination of cells that are no longer needed in an organism (*1*). During the past few years, there has been growing support for the idea that the basic molecular mechanism underlying apoptosis has been conserved during evolution among animals as diverse as nematodes, insects, and mammals (*2*). A central step in this cell suicide pathway is the activation of an unusual class of cysteine proteases, named caspases (*3*), that includes mammalian interleukin-1β–converting enzyme (ICE) and the *ced-3* gene of nematodes (*4*). Caspases are synthesized as inactive zymogens that need to be processed to form active heterodimeric enzymes (*4*). However, the precise mechanism of caspase activation in response to apoptotic stimuli remains unknown. Likewise, with the exception of the *Caenorhabditis elegans* caspase CED-3, it is not clear what precise role any other caspase has in apoptosis.

The availability of many sophisticated genetic and molecular techniques makes *Drosophila* ideally suited for studying the questions of caspase activation and function. In *Drosophila*, like in mammalian systems, the onset of apoptosis is regulated by a number of distinct death-inducing stimuli (*5*). Genetic studies have led to the identification of three apoptotic activators, *reaper* (*6*), *head involution defective (hid)* (*7*), and *grim* (*8*), that appear to act as mediators between different signaling pathways and the cell death program. The deletion of all three genes blocks apoptosis in *Drosophila* (*6*), and overexpression of any one of them is sufficient to kill cells that would normally live (*7–9*). The products of these genes appear to activate one or more caspases, because cell killing by *reaper*, *hid*, and *grim* is blocked by the baculovirus protein p35 (*7–9*), a specific inhibitor of caspases (*10*).

To gain further insight into the function and control of caspase activity, we isolated *Drosophila* caspase-like sequences. Degenerate oligonucleotides corresponding to two highly conserved regions flanking the active site of the enzyme were designed and used for a polymerase chain reaction (PCR) with a *Drosophila* 4- to 8-hour embryo cDNA library as the template (*11*). We obtained several PCR products of the expected size that were subcloned and sequenced (*11*). One clone was highly homologous to the region containing the caspase active site, including the highly conserved QACRG (*12*) pentapeptide. This clone was used to isolate full-length cDNA clones and to deduce the entire amino acid sequence of this putative caspase (*11*). The predicted open reading frame of the full-length cDNA encodes a protein of 323 amino acids (Fig. 1A). The DNA sequence surrounding the first ATG (CAAGATGACC) is in good agreement with the consensus sequence for translation initiation in *Drosophila* (*13*). The corresponding protein was named *Drosophila* caspase-1 (DCP-1). In comparison with other caspase family members (*4*, *14–16*), DCP-1 is more homologous to CPP-32 and MCH-2α than to ICE. It shares 37% sequence identity with both CPP-32 and MCH-2α, 29% identity with NEDD-2 (ICH-1), 28% with CED-3, and 25% with human ICE. This sequence similarity suggests that DCP-1 may be a member of the *ced-3*–CPP-32 subfamily of caspases.

Caspases are synthesized as inactive proenzymes that are proteolytically processed to form the active heterodimer consisting of a p10 (10 kD) and a p20 (20 kD) subunit (*4*). The consensus sequence for proteolysis of many *ced-3*–like caspases is (D/E)XXD-Y (*12*), where X can be any amino acid and Y is a small amino acid, such as Ala, Gly, or Ser. Cleavage occurs

Howard Hughes Medical Institute, Department of Brain and Cognitive Sciences and Department of Biology, Massachusetts Institute of Technology, Cambridge, MA 02139, USA.

*To whom correspondence should be addressed.

between Asp and Y. A good match to this consensus, DNTD-A, is found in the expected region of DCP-1, indicating that cleavage may occur between Asp[33] and Ala[34]. This prediction was supported by the biochemical properties of a truncated version of DCP-1 (discussed below). Therefore, like CPP-32 and MCH-2α, DCP-1 appears to have a short prodomain of only 33 amino acids. On the basis of the x-ray crystal structure of ICE (*17*), it is thought that Cys[285], His[237], and Gly[238] in this molecule are involved in the catalysis of the peptide cleavage, whereas Arg[179], Gln[283], Arg[341], and Ser[347] are involved in the recognition of the Asp at the P1 position. All the corresponding amino acid residues are conserved in DCP-1 (Fig. 1B) and in other family members. DCP-1 contains a slightly modified pentapeptide, QACQG, instead of the more common QACRG, which is also found in mammalian Mch4 and Mch5 (also called MACH or FLICE) (*16*).

To show that DCP-1 protein has protease activity, we expressed two different versions in *Escherichia coli* and tested the biochemical activity of the recombinant proteins on known substrates for caspases (*18*). Full-length DCP-1 gave no or very little activity, whereas a truncated protein lacking the putative prodomain had very strong protease activity. This form of DCP-1 cleaved both poly(adenosine diphosphate–ribose) polymerase (PARP) (Fig. 2A) and p35 into fragments of the predicted size. Direct comparison with fragments generated by CED-3 cleavage indicated that both proteases cleave at identical sites (Fig. 2A). DCP-1 protease activity was completely abolished by iodoacetamide; thus cysteine is critical for enzyme activity. The CPP-32–specific inhibitor Ac-DEVD-CHO (*14*) completely inhibited PARP cleavage by DCP-1, whereas the ICE-specific inhibitor Ac-YVAD-CHO was ineffective (Fig. 2A). Therefore, DCP-1 is biochemically more closely related to CED-3 and CPP-32 than to ICE. DCP-1 also cleaved p35 in a manner identical to that of CED-3. Finally, the composition of the autoprocessed mature DCP-1 enzyme was determined. After purification of the truncated form of DCP-1, two bands of about 22 kD (corresponding to p20) and 13 kD (corresponding to p10) were detected with SDS–polyacrylamide gel electrophoresis (PAGE). Microsequencing analysis of the small subunit (*19*) demonstrated that the cleavage site producing the two subunits was, as expected, between Asp[215] and Gly[216] (Fig. 1B). These results show that DCP-1 is a cysteine protease and has biochemical properties that are similar to that of the *C. elegans* cell death protease CED-3.

To determine if DCP-1 can induce cell death, we expressed the gene in several mammalian cell lines (*20*). Cells expressing DCP-1 displayed the typical apoptotic morphology, such as condensed, rounded cell morphology and severe membrane blebbing. These observations indicate that expression of DCP-1 is sufficient to induce apoptosis. However, because expression of several proteases, including proteinase K, trypsin, and chymotrypsin, can induce apoptosis (*21*), DCP-1 may kill by causing cellular damage that subsequently triggers an apoptotic response. To eliminate this possibility, we used a cell-free apoptosis system that permits the investigation of apoptosis-like nuclear events (*22*). In this system, cellular structures have been destroyed and therefore are no longer capable of sensing

A

```
MTDECVTRNY GVGIRSPNGS ENRGSFIMAD NTDAKGCTPE SLVVGGATAA  50
SPLPANKFVA RMPVERYASE YNMSHKHRGV ALIFNHEFFD IPSLKSRTGT 100
NVDAQELKKA FENLGFAVSV HKDCKLRDIL KHVGKAAELD HTDNDCLAVA 150
ILSHGEHGYL YAKDTQYKLD NIWHYFTATF CPSLAGKPKL FFIQACQGDR 200
LDGGITLEKG VTETDGESST SYKIPIHADF LFSYSTIPGY FSWRNINNGS 250
WYMQSLIREL NANGKKYDLL TLLTFVNQRV ALDFESNVPA TPMMDRQKQI 300
PCLTSMLTRI LRFGDKPNGN KAG
```

B

```
      <------------------ Large subunit ------------------>|<--- Small subunit --->
DCP-1 KSRTGTNVD..LSHGEH..CPSLAGKPKLFFIQACQGDR..TETDG..GYFSWRNINNGSWYMQSLI
Mch5  RDRNGTHLD..LSHGDK..CPSLAGKPKVFFIQACQGDN..VETDS..NCVSYRNPAEGTWYIQSLC
Mch4  KDRQGTHKD..LTHGRF..CPRLAEKPKLFFIQACQGEE..IEADA..GYVSFRHVEEGSWYIQSLC
Mch2  PERRGTCAD..LSHGEG..CHSLVGKPKIFIIQACRGNQ..TEVDA..GYYSHRETVNGSWYIQDLC
CPP32 TSRSGTDVD..LSHGEE..CRSLTGKPKLFIIQACRGTE..IETDS..GYYSWRNSKDGSWFIQSLC
CED-3 PTRNGTKAD..LSHGEE..APRLANKPKIVFVQACRGER..DSVDG..QYVSWRNSARGSWFIQAVC
ICE   PRRTGAEVD..MSHGIR..CPSLKDKPKVIIIQACRGDS..WFKDS..DNVSWRHPTMGSVFIGRLI
ICH-1 EFRSGGDVD..LSHGVE..CPSLQNKPKMFFIQACRGDE..DQQDG..GTAAMRNTKRGSWYIEALA
          ○         □□                ○ □                      ○     ○
          179   237 238              283 285                   341   347
```

Fig. 1. Predicted amino acid sequence of DCP-1 and its homology to other caspase family members (*12*). (**A**) Predicted amino acid sequence of DCP-1. The putative prodomain contains the NH_2-terminal 33 amino acids that appear to be removed by proteolytic cleavage at DNTDA (*12*), between Asp[33] and Ala[34]. The cleavage site that generates the large and small subunits is at TETDG, between Asp[215] and Gly[216]. Another possible cleavage site, DRLDG, is between Asp[202] and Gly[203]. The active site QACQG is in bold face, and putative cleavage sites are underlined. (**B**) Sequence alignment of the most conserved regions among several caspases. The active site pentapeptide is boxed. The cleavage site that generates the large (p20) and small (p10) subunit in DCP-1 is between Asp[215] and Gly[216]. Dotted lines indicate gaps in the sequence to allow optimal alignment. MACH (FLICE) shares identical sequence with Mch5 in the listed regions, therefore it is not shown here. The crystal structure of ICE indicates that Cys[285], His[237], and Gly[238] (□) are involved in the catalysis, and Arg[179], Gln[283], Arg[341], and Ser[347] (○) are involved in the recognition of the P1 Asp. All these residues are conserved among these proteins except one close substitution of Ser to Thr in Mch5.

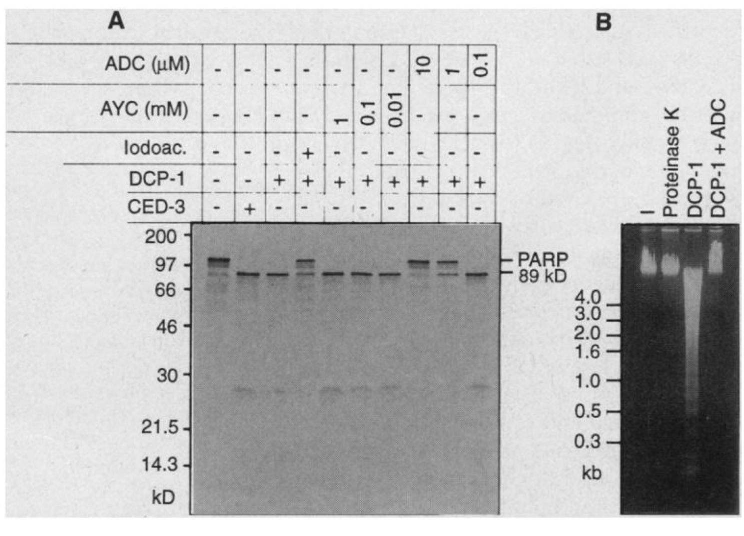

Fig. 2. DCP-1 has caspase activity and induces DNA fragmentation in HeLa cell nuclei. (**A**) DCP-1 cleaves PARP, and this activity can be inhibited by iodoacetamide (Iodoac.) and Ac-DEVD-CHO (ADC), but not by the ICE inhibitor Ac-YVAD-CHO (AYC). ^{35}S-labeled human PARP (hPARP) was used as the substrate for protease activity analysis. For inhibition, 10 mM iodoacetamide, Ac-DEVD-CHO, or Ac-YVAD-CHO, as indicated, was used as an inhibitor. They were mixed and incubated with the enzyme at 37°C for 10 min. Then ^{35}S-labeled hPARP was added and incubated at 37°C for 30 min. CED-3 protein was used as control and PARP cleavage was analyzed by 10% SDS-PAGE. (**B**) DCP-1 induces DNA fragmentation in HeLa cell nuclei. Methods are described in (*22*).

physiological signals. Purified DCP-1 or proteinase K as a control was added to such a cell-free preparation from HeLa cells (*22*). Upon treatment with DCP-1, the chromosomal DNA was fragmented and displayed the characteristic apoptotic DNA ladder (Fig. 2B). In contrast, proteinase K failed to induce DNA fragmentation in this system (Fig. 2B). Thus, DCP-1 acts far downstream to induce apoptosis, either by directly cleaving apoptotic targets or by activating other procaspases that may be present in the cell-free system. In either case, the fact that a *Drosophila* protein, DCP-1, can engage at least part of the apoptotic program in mammalian cells suggests that its targets have been conserved in evolution.

A *Drosophila* cell death caspase should be expressed in all cells that have the ability to undergo apoptosis. We determined the distribution of *dcp-1* mRNA during *Drosophila* embryogenesis by in situ hybridization (*23*). Preblastoderm embryos, a stage before the onset of zygotic transcription, contained large and uniform amounts of *dcp-1* RNA (Fig. 3A). Therefore, *dcp-1* is maternally expressed. In later stages, *dcp-1* transcripts continued to be present throughout the embryo (Fig. 3B). This uniform pattern of RNA distribution is consistent with a role of *dcp-1* as an apoptotic effector. Toward the end of embryogenesis, *dcp-1* expression became more restricted (Fig. 3C). The reduction of *dcp-1* transcript correlated well with the increased resistance of late embryos to the induction of apoptosis by x-ray irradiation and ectopic expression of *reaper* (*9*).

To begin investigating the function of DCP-1, we obtained loss-of-function mutations in the gene. *dcp-1* was mapped by in situ hybridization to the cytological position 59F on the right arm of chromosome II, and chromosomal deletions for this locus were identified (*24*) (Fig. 4). In addition, two preexisting lethal *P* element insertions, l(2)01862 and l(2)02132, were found to be inserted at different positions in the first exon of *dcp-1* (Fig. 4) (*24*). These *P* element mutants behaved genetically as null alleles and will be referred to as the $dcp\text{-}1^{1862}$ and $dcp\text{-}1^{2132}$ alleles. Viable revertants of these alleles were generated and were associated with *P* element excisions, demonstrating that the phenotypes described below are indeed caused by the transposon insertions into the *dcp-1* gene (*25*). To eliminate possible contributions of other mutations in the genetic background of the *dcp-1 P* element alleles, we conducted phenotypic analyses in trans to a deletion for *dcp-1* (*26*).

Because *ced-3* mutants of *C. elegans* are defective in programmed cell death, we investigated the pattern of apoptosis in embryos lacking zygotic *dcp-1* function. Using TUNEL labeling and ENGRAILED antibody staining, we detected no significant abnormalities in the pattern of cell death (*27*). These data indicate that zygotic DCP-1 function is not required for most embryonic cell deaths in *Drosophila*, perhaps because of the existence of additional caspases (*28*). However, because DCP-1 has significant maternal expression, it is also possible that sufficient DCP-1 protein is present during embryogenesis for cell death to occur.

Both alleles of *dcp-1* caused lethality during larval stages, showing that *dcp-1* is an essential gene. This lethality was associated with the transposon insertions, because it was seen in transheterozygotes of the two different *P* insertions and because it could be reverted by excision of the *P* elements (*25*). Although most of the *dcp-1* homozygotes died before the third instar larval stage, some of the *dcp-1* homozygotes reached that stage and displayed several abnormalities. Larvae mutant for *dcp-1* had an overall normal central nervous system but lacked imaginal discs and gonads. In addition, they had fragile trachea. However, the most prominent phenotype of these larvae was the presence of melanotic tumors, located in various parts of the body (Fig. 5). Melanotic tumors can result from either the overproliferation of blood cells or from an immune response toward abnormal cells and tissues in the larva (*29*). In *dcp-1* mutants, no evidence for hyperplasia of the lymph glands or overproliferation of blood cells was found. This suggests an immune reaction toward abnormal tissues or cells, possibly resulting from a defect in cell death. According to this model, cells that would have normally been eliminated by apoptosis persist in DCP-1–deficient animals but are eventually recognized by the fly's immune system. Although mammalian caspases have not yet been implicated in tumor suppression, this scenario would be consistent with the known role of apoptosis

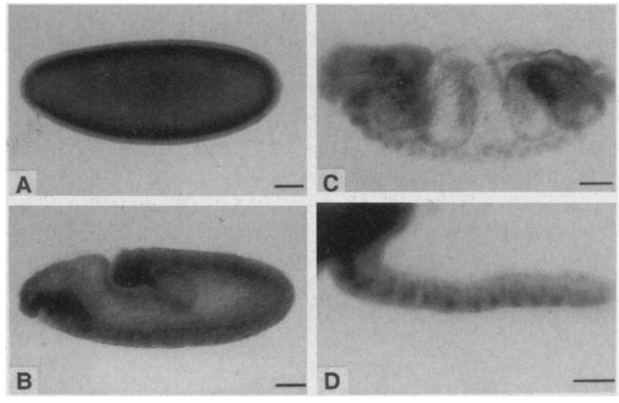

Fig. 3. *dcp-1* mRNA expression in *Drosophila* embryos. Whole mount wild-type embryos were hybridized with a *dcp-1* digoxigenin-labeled probe (*23*). (**A**) Stage 4 embryo (*31*). Uniform mRNA distribution was observed in all embryos before cell formation and the onset of zygotic transcription (stages 1 to 5), demonstrating that *dcp-1* is maternally expressed. (**B**) Stage 10 embryo (*31*). *dcp-1* transcripts were found in essentially all cells during germband extension. The weakly stained central region of the embryo contains mainly yolk. (**C**) Stage 16 embryo (*31*). The expression of *dcp-1* became nonuniform in advanced stages of embryogenesis. Although low levels of transcript appeared to be still present throughout the embryo, some regions of the embryo, including the head, some cells within the central nervous system, the developing gonads, and a portion of the gut, were strongly labeled. (**D**) Lateral view of the central nervous system of a stage 17 embryo (*31*). Strong expression of *dcp-1* was seen in cells along the midline of the central nervous system. Scale bars are 50 μm.

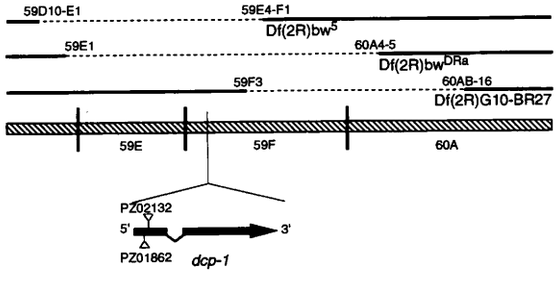

Fig. 4. Map of the 59F region. The hatched bar represents the wild-type chromosome, and the cytological divisions are indicated. The deletion strains used for in situ analysis are drawn above the hatched bar, with the dashed lines representing the deleted regions. They are labeled with their reported breakpoints (*24*). Genetic analysis with a number of lethals that map to the region revealed that $Df(2R)bw^5$ and Df(2R)G10-BR27 may overlap, because both deletions fail to complement at least one lethal complementation group. The approximate position of the *dcp-1* gene is indicated below the hatched bar; the orientation is drawn arbitrarily as it has not yet been determined. The genomic DNA 3′ of the *P* elements has been partially sequenced, revealing a 430–base pair intron. The *P* elements are inserted in exonic sequences 182 and 291 base pairs downstream of the start of the cDNA and 179 and 70 base pairs upstream of the initiation codon.

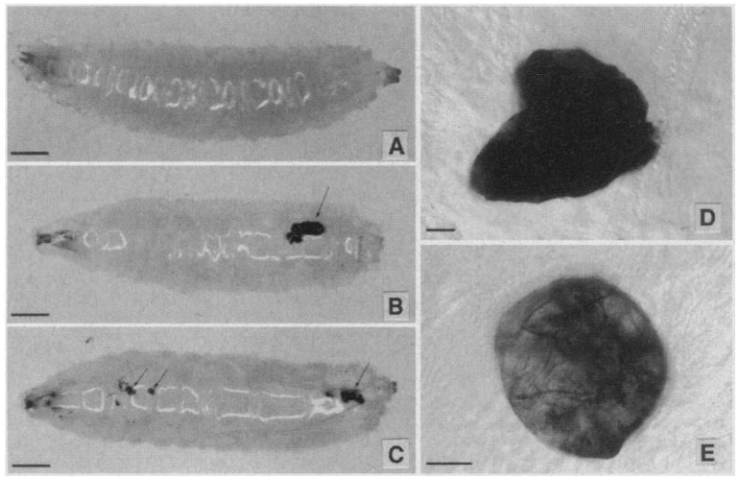

Fig. 5. Melanotic tumor phenotype of *dcp-1* mutants. (**A**) A wild-type (Canton S) larva at the wandering third instar stage (~5 days). (**B** and **C**) *dcp-1*^{1862}/*Df(2R)bw*^{DRa} transheterozygous larvae (~11 to 12 days). The conspicuous dark masses, indicated by arrows, are the melanotic tumors that occur in various locations in the larvae. Scale bars in (A), (B), and (C) are 500 μm. (**D** and **E**) Higher magnification view of two melanotic tumors from a *dcp-1*^{1862}/*Df(2R)bw*^{DRa} larva. Scale bars are 50 μm.

in preventing tumorigenesis in mammals (*30*). Alternatively, the lack of *dcp-1* function may lead to the aberrant differentiation of certain cells to a state where they become recognized as "nonself." In this case, *dcp-1* would have a novel function that is independent and distinct from a role in cell death. This possibility is supported by the tracheal and imaginal disc phenotypes that are not easily explained by defects in programmed cell death.

The existence of prominent, fully penetrant phenotypes in *dcp-1* mutants should facilitate future investigations on whether caspases may indeed have important and currently unknown developmental functions. Because *Drosophila* contains multiple caspases (*28*), it will also be possible to investigate whether these proteases function in a cascade or in parallel pathways or have redundant functions. Additionally, it should now be possible to identify functionally relevant targets of these proteases by the use of genetic as well as biochemical means. Finally, the identification of *Drosophila* caspases should help elucidate the mechanism by which they are regulated in response to apoptotic activators, such as *reaper*, *hid*, and *grim*. Because these genes provide a crucial link between different death-inducing signaling pathways and caspase activation, it should eventually be possible to deduce the precise mechanism by which defined apoptotic stimuli activate the cell death program.

REFERENCES AND NOTES

1. R. E. Ellis, J. Yuan, H. R. Horvitz, *Annu. Rev. Cell Biol.* **7**, 663 (1991); M. C. Raff, *Nature* **356**, 397 (1992); M. C. Raff *et al.*, *Science* **262**, 695 (1993); H. Steller, *ibid.* **267**, 1445 (1995).
2. D. L. Vaux, G. Haecker, A. Strasser, *Cell* **76**, 777 (1994); J. C. Ameisen, *Science* **272**, 1278 (1996); M. O. Hengartner, *Curr. Opin. Genet. Dev.* **6**, 34 (1996).
3. E. S. Alnemri *et al.*, *Cell* **87**, 171 (1996).
4. D. P. Cerretti *et al.*, *Science* **256**, 97 (1992); N. A. Thornberry *et al.*, *Nature* **356**, 768 (1992); J. Yuan *et al.*, *Cell* **75**, 641 (1993); S. Kumar, *Trends Biochem. Sci.* **20**, 198 (1995); A. Takahashi and W. C. Earnshaw, *Curr. Opin. Genet. Dev.* **6**, 50 (1996); D. Xue *et al.*, *Genes Dev.* **10**, 1973 (1996).
5. S. Robinow *et al.*, *Development* **119**, 1251 (1993); J. M. Abrams *et al.*, *ibid.* **117**, 29 (1993); H. Steller and M. E. Grether, *Neuron* **13**, 1269 (1994).
6. K. White *et al.*, *Science* **264**, 677 (1994).
7. M. E. Grether, J. M. Abrams, J. Agapite, K. White, H. Steller, *Genes Dev.* **9**, 1694 (1995).
8. P. Chen, W. Nordstrom, B. Gish, J. M. Abrams, *ibid.* **10**, 1773 (1996).
9. K. White, E. Tahaoglu, H. Steller, *Science* **271**, 805 (1996).
10. N. J. Bump *et al.*, *ibid.* **269**, 1885 (1995); D. Xue and H. R. Horvitz, *Nature* **377**, 248 (1995).
11. Degenerate oligonucleotides corresponding to two highly conserved region upstream (LSHGEE) and downstream (GSWFIQ) from the caspase active site (QACRG) were used to perform PCR. Two degenerate primers encoding LSHGEE (CTG TCI CAT/C GGI GAA/G GA and CTG AGC/T CAT/C GGI GAA/G GA) and two backward primers encoding GSWFIQ (CTG G/AAT GAA CCA IGA ICC and CTG G/AAT GAA CCA G/ACT ICC) were used in standard PCR reactions with an annealing temperature of 40°C and 0.5 μg of DNA from a 4- to 8-hour *Drosophila* embryo cDNA library [N. H. Brown and F. C. Kafatos, *J. Mol. Biol.* **203**, 425 (1988)] as the template. PCR products with a size of 300 to 400 base pairs (bp) were reamplified and cloned into a Sma I–cut Bluescript II KS vector. Inserts were sequenced with ^{35}S-labeled deoxyadenosine triphosphate (dATP) and the DNA sequencing kit (United States Biochemical). A ^{32}P-labeled DNA probe was synthesized by PCR with the same PCR primers and used to isolate full-length cDNA clones from the aforementioned cDNA library. From screening 10^6 cDNA clones, 12 identical clones for *dcp-1* were obtained and sequenced.
12. Single-letter abbreviations for the amino acid residues are A, Ala; C, Cys; D, Asp; E, Glu; F, Phe; G, Gly; H, His; I, Ile; K, Lys; L, Leu; M, Met; N, Asn; P, Pro, Q, Gln; R, Arg; S, Ser; T, Thr; V, Val; W, Trp; and Y, Tyr.
13. D. R. Cavener, *Nucleic Acids Res.* **15**, 1353 (1987).
14. D. W. Nicholson *et al.*, *Nature* **376**, 37 (1995).
15. T. Fernandez-Alnemri *et al.*, *J. Biol. Chem.* **269**, 30764 (1994); M. Tewari *et al.*, *Cell* **81**, 801 (1995); T. Fernandez-Alnemri *et al.*, *Cancer Res.* **55**, 2737 (1995); T. Fernandez-Alnemri *et al.*, *ibid.*, p. 6045; J. A. Lipke *et al.*, *J. Biol. Chem.* **271**, 1825 (1996); H. Duan *et al.*, *ibid.*, p. 1621; L. Wang *et al.*, *Cell* **78**, 739 (1994); S. Kumar *et al.*, *Genes Dev.* **8**, 1613 (1994); J. Kamens *et al.*, *J. Biol. Chem.* **270**, 15250 (1995); C. Faucheu *et al.*, *EMBO J.* **14**, 1914 (1995); N. A. Munday *et al.*, *J. Biol. Chem.* **270**, 15870 (1995); H. Duan *et al.*, *ibid.* **271**, 16720 (1996); K. Kuida *et al.*, *Science* **267**, 2000 (1995); P. Li *et al.*, *Cell* **80**, 401 (1995).
16. M. P. Boldin *et al.*, *Cell* **85**, 803 (1996); M. Muzio *et al.*, *ibid.*, p. 817; T. Fernandes-Alnemri *et al.*, *Proc. Natl. Acad. Sci. U.S.A.* **93**, 7464 (1996).
17. N. P. C. Walker *et al.*, *Cell* **78**, 343 (1994); K. P. Wilson *et al.*, *Nature* **370**, 270 (1994).
18. Different forms of recombinant DCP-1 protein containing COOH-terminal His_6 tags were expressed in *Escherichia coli* by cloning PCR-generated constructs into pET3a (Novagen). Proteins were purified with Ni^{2+} columns (Novagen) by following the manufacturer's instructions. The protease activity of different forms of DCP-1 was assayed by incubating the recombinant protein with well-characterized targets for caspases, such as PARP [S. H. Kaufmann *et al.*, *Cancer Res.* **53**, 3976 (1993); Y. A. Lazebnik *et al.*, *Nature* **371**, 346 (1994)] and p35. For this purpose, ^{35}S-labeled PARP and p35 were prepared by in vitro translation with the TNT-coupled reticulocyte lysate system (Promega). For each cleavage reaction, 0.2 μl of partially purified DCP-1 was added to 4 μl of reaction buffer [25 mM Hepes, 5 mM EDTA, 2 mM dithiothreitol (DTT), 0.1% CHAPS, pH 7.5]. For inhibition, 1 μl of iodoacetamide, Ac-DEVD-CHO, or Ac-YVAD-CHO (Enzyme Systems Products, Dublin, CA) was added to reach the final concentration. These mixtures were incubated at 37°C for 10 min. Then 0.5 μl of ^{35}S-labeled hPARP was added and incubated at 37°C for 30 min. In both experiments, CED-3 protein was used as a control. PARP cleavage was analyzed with 10% SDS-PAGE, and p35 cleavage was analyzed with 15% SDS-PAGE.
19. A truncated version of DCP-1 purified on a Ni^{2+} column was subjected to 12% SDS-PAGE. The separated protein bands were electrophoretically blotted onto polyvinylidene difluoride membrane (Bio-Rad) and stained with Coomassie Brilliant Blue R-250. After destaining, the small subunit (13 kD) was cut off and microsequenced at the Biopolymers Laboratory (Massachusettes Institute of Technology). The NH_2-terminal amino acid sequence was as follows: GESSTSYKIPIHADFLFSYSTIPGYFSWRNINN (*12*), indicating that the cleavage site to give rise to two subunits is between Asp^{215} and Gly^{216}.
20. We basically followed the method of M. Miura *et al.*, *Cell* **75**, 653 (1993). The full-length version of DCP-1 was generated by PCR with the upstream primer (5′-GCGGAGTCGACGATGACCGACGAGTGCGTA-3′) and the downstream primer (5′-CGGATCCGTCGACGCGCCAGCCTTATTGCCGTT-3′) that both have a Sal I site. After treatment with Sal I, the PCR product was cloned into the Sal I–treated, dephosphorylated mammalian expression vector pactβgal (provided by J. Yuan). Clones with the correct orientation were identified by sequencing. Cells were transiently transfected with 1 μg of DNA and 8 μl of lipofectamine reagent (Gibco-BRL), following the manufacturer's instructions.
21. M. S. Williams and P. A. Henkart, *J. Immunol.* **153**, 4247 (1994).
22. Several cell-free apoptosis models have been previously used to study caspases [Y. A. Lazebnik *et al.*, *J. Cell Biol.* **123**, 7 (1993); K. Orth *et al.*, *J. Biol. Chem.* **271**, 20977 (1996); M. Enari *et al.*, *Nature* **380**, 723 (1996)]. We essentially followed the protocol of M. Enari *et al.* In our experiments, 0.3 ml of packed HeLa cells was homogenized in 1 ml of buffer [10 mM Hepes, pH 7.0, 40 mM β-glycerophosphate, 50 mM NaCl, 2 mM $MgCl_2$, 5 mM EGTA, 1 mM DTT, 2 mM ATP, 10 mM creatine phosphate, creatine kinase (50 μg/ml), and bovine serum albumin (0.2 mg/ml)] until more than 95% of the cells

were broken but nuclei remained intact when analyzed under a microscope. A 30-μl sample of this homogenate was used for each assay. To the homogenate was added 1 μl (0.1 μg) of proteinase K or 1 μl of partially purified DCP-1. For inhibition of DCP-1, 0.1 mM Ac-DEVD-CHO was added with DCP-1. After 3 hours of incubation at 37°C, DNA was extracted and analyzed by agarose gel electrophoresis.

23. In situ hybridizations were performed as described (6).
24. Chromosome in situ analysis was performed essentially as described [M. Ashburner, Drosophila: *A Laboratory Manual* (Cold Spring Harbor Laboratory, Cold Spring Harbor, NY, 1989), protocol 27]. A DCP-1 biotinylated probe was hybridized to the wild type as well as the three deletion strains shown in Fig. 4. A collection of preexisting *P* element insertions mapping to the 59E-F region were crossed to these deletion strains for complementation analysis and were further analyzed by Southern (DNA) blot hybridization. Two *P* element strains, l(2)02132 and l(2)01862, showed alterations on a Southern blot when probed with the DCP-1 cDNA. The position and orientation of the two *P* elements in the DCP-1 gene were confirmed by PCR by using a 3′ *P* element primer and a primer within the DCP-1 coding region, and DNA sequencing of the PCR products. The Df(2R)G10-BR27 and Df(2R)bw^{DRa} stocks were received from B. Reed. *P* element strains were generated by the Berkeley *Drosophila* Genome Project and, together with Df(2R)bw^{5}, provided by the Bloomington Stock Center.
25. *P* element revertants were generated by standard genetic techniques. Viable and lethal revertants were recovered for both of the *P* element lines. Southern blot analysis was used to determine the presence of the *P* elements in the revertant lines.
26. Phenotypic analyses were performed on *dcp-1^{1862}/Df(2R)bw^{DRa}* transheterozygotes. These animals survive to various stages of larval development and display the melanotic tumor phenotype. The same phenotypes were also observed in *dcp-1^{1862}/dcp-1^{2132}* heterozygotes, and in larvae homozygous for a single transposon insertion. However, the *dcp-1^{1862}* chromosome appeared to contain additionally an unrelated background mutation that caused dorsal cuticle defects in embryos.
27. TUNEL labeling was carried out as described (9). This technique labels apoptotic nuclei by incorporating biotinylated nucleotides at the end of DNA double-strand breaks [Y. Gavrieli *et al.*, *J. Cell. Biol.* **119**, 493 (1992)]. In addition, antibody staining against the ENGRAILED protein was used to check for the presence of supernumerary cells in the CNS [L. Zhou *et al.*, *Curr. Biol.* **5**, 784 (1995)].
28. Z. Song and H. Steller, unpublished observations; A. Fraser and G. Evan, personal communication.
29. K. L. Watson *et al.*, *Dev. Genet.* **12**, 173 (1991); J. Sparrow, in *The Genetics and Biology of* Drosophila *2b*, M. Ashburner and T. R. Wright, Eds. (Academic Press, New York, 1978).
30. C. B. Thompson, *Science* **267**, 1456 (1995).
31. J. Campos-Ortega and V. Hartenstein, *The Embryonic Development of* Drosophila melanogaster (Springer-Verlag, New York, 1985).
32. We thank J. Yuan for providing the pactβgal vector and suggestions; D. Xue for a gift of CED-3 protein and advice; C. Hynds for assistance with figures; B. Reed, K. Matthews, and the Bloomington Stock Center for *Drosophila* stocks; the Berkeley *Drosophila* Genome Project for information on the *P* element strains; and K. Watson and C. Dearolf for useful advice. Supported by the American Cancer Society (K.M.). Z.S. is a postdoctoral associate and H.S. is an associate investigator of the Howard Hughes Medical Institute.

15 October 1996; accepted 3 December 1996

Requirement for the Transcription Factor LSIRF/IRF4 for Mature B and T Lymphocyte Function

Hans-Willi Mittrücker, Toshifumi Matsuyama, Alex Grossman, Thomas M. Kündig, Julia Potter, Arda Shahinian, Andrew Wakeham, Bruce Patterson, Pamela S. Ohashi, Tak W. Mak*

Lymphocyte-specific interferon regulatory factor (LSIRF) (now called IRF4) is a transcription factor expressed only in lymphocytes. Mice deficient in IRF4 showed normal distribution of B and T lymphocyes at 4 to 5 weeks of age but developed progressive generalized lymphadenopathy. IRF4-deficient mice exhibited a profound reduction in serum immunoglobulin concentrations and did not mount detectable antibody responses. T lymphocyte function was also impaired in vivo; these mice could not generate cytotoxic or antitumor responses. Thus, IRF4 is essential for the function and homeostasis of both mature B and mature T lymphocytes.

Lymphocyte-specific interferon regulatory factor (LSIRF) [now called IRF4 (*1*)] is a lymphocyte-restricted member of the interferon regulatory factor (IRF) family of transcription factors (*2*–*4*). This family is defined by a characteristic DNA binding domain and the ability to bind to the interferon-stimulated response element. Members of the IRF family are involved in diverse processes such as pathogen response, cytokine signaling, apoptosis, and control of cell proliferation (*5*).

We generated mice deficient in IRF4 by replacing exons 2 and 3 of the IRF4 gene with a neomycin resistance gene (*6*). Mouse strains derived from two independent embryonic stem cell lines exhibited an identical phenotype. Mutation of the IRF4 gene was confirmed by Southern (DNA) blot analysis of tail DNA (shown for one mouse strain in Fig. 1A). Hind III–digested DNA from IRF4$^{+/-}$ and IRF4$^{-/-}$ mice displayed the 3.3-kb band of the mutant locus; the wild-type band at 8.4 kb was absent in IRF4$^{-/-}$ mice. The absence of the IRF4 protein was confirmed by protein immunoblot analysis (Fig. 1B).

At 4 to 5 weeks of age, lymph nodes and spleens of IRF4$^{-/-}$ mice showed a relatively normal lymphocyte distribution and cellularity as compared with those of control littermates (Fig. 1C). At 10 to 15 weeks, spleens were enlarged 3 to 5 times and lymph nodes were enlarged 10 times over those of control littermates, because of an expansion of T (both CD4^{+} and CD8^{+}) and B lymphocytes (Fig. 1C). The distribution of several different V_{β}-elements of the TCR was conserved, excluding the expansion of single T cell clones. Analysis of T cell surface molecules, including CD2, CD11a, CD18, CD25, CD28, CD45, CD54, FAS, and Thy-1, did not reveal any changes, although a slight increase in the number of CD69^{+} T cells was observed. Thymi of IRF4$^{-/-}$ mice were of normal size and showed a normal distribution of thymic cell populations (Fig. 1C) (*7*).

Analysis of B lymphocytes from bone marrow revealed no differences in the expression of the B cell surface molecules CD43, immunoglobulin M (IgM), IgD, Igκ, B220, and I-A, indicating that early B cell development was grossly normal. The development of peritoneal CD5^{+} B1 B cells was also normal (*7*). Splenic B cells showed normal surface expression of IgM and of κ and λ light chains (Fig. 2). However, on closer examination, spleens from IRF4$^{-/-}$ mice were found to display increased membrane IgM (mIgM)^{high} mIgD^{low}, and decreased mIgM^{low} mIgD^{high}, B cell populations. The frequency of CD23^{+} B220^{+} B cells was markedly reduced, and the CD23^{high} B220^{+} B cell subpopulation was absent (Fig. 2), indicating a block at a late stage of peripheral B cell maturation (*8*). Consistent with such a block was the absence of germinal centers in B cell follicles of spleens and lymph nodes, even after the injection of sheep red blood cells, a stimulus that induces a large number of germinal centers in control mice (*9*). Furthermore, plasma cells could not be detected in the spleen or lamina propria of IRF4$^{-/-}$ mice.

H.-W. Mittrücker, A. Grossman, T. M. Kündig, J. Potter, A. Shahinian, A. Wakeham, P. S. Ohashi, T. W. Mak, Departments of Immunology and Medical Biophysics, University of Toronto, and the Amgen Institute, 610 University Avenue, Toronto, Ontario, M5G 2C1, Canada.
T. Matsuyama, Department of Oncology, Faculty of Medicine, Nagasaki University, Nagaskai, Japan.
B. Patterson, Department of Oncologic Pathology, Ontario Cancer Institute, 610 University Avenue, Toronto, Ontario, M5G 2C1, Canada.
*To whom correspondence should be addressed.